Plasmonic Photocatalysis

International Edition: DOI: 10.1002/anie.201412030
German Edition: DOI: 10.1002/ange.201412030

Probing Long-Lived Plasmonic-Generated Charges in TiO_2/Au by High-Resolution X-ray Absorption Spectroscopy**

Lucia Amidani, Alberto Naldoni,* Marco Malvestuto, Marcello Marelli, Pieter Glatzel, Vladimiro Dal Santo, and Federico Boscherini*

Abstract: *Exploiting plasmonic Au nanoparticles to sensitize TiO_2 to visible light is a widely employed route to produce efficient photocatalysts. However, a description of the atomic and electronic structure of the semiconductor sites in which charges are injected is still not available. Such a description is of great importance in understanding the underlying physical mechanisms and to improve the design of catalysts with enhanced photoactivity. We investigated changes in the local electronic structure of Ti in pure and N-doped nanostructured TiO_2 loaded with Au nanoparticles during continuous selective excitation of the Au localized surface plasmon resonance with X-ray absorption spectroscopy (XAS) and resonant inelastic X-ray scattering (RIXS). Spectral variations strongly support the presence of long-lived charges localized on Ti states at the semiconductor surface, giving rise to new laser-induced low-coordinated Ti sites.*

The search for innovative and efficient schemes for the use of solar energy is motivated by the increasing demand for clean energy. Materials used in artificial photosynthesis, for example, in water splitting/CO_2 reduction,[1,2] also find application in important chemical processes, such as wastewater treatment, pollutant removal, and production of fine chemicals.[3,4]

Wide band gap semiconductors, that is, TiO_2, have a low conversion efficiency owing to their poor absorption of solar light. Among the new concepts introduced to increase light harvesting, the use of plasmonics is particularly promising.[3] Plasmonic nanoparticles (NPs) have extremely high absorption cross-sections as a result of localized surface plasmon resonance (LSPR), which is easily tailored across the solar spectrum by the NPs shape and size. Upon illumination, plasmonic NPs can sensitize semiconductors to below band-gap light and create charge-separated states with prolonged lifetime.[4] The main sensitization mechanism is the generation of hot electrons (e^-) which have sufficient energy to overcome the Schottky barrier at the metal/TiO_2 interface and be injected into the TiO_2 conduction band (CB). In parallel, the unique ability of plasmonic NPs to concentrate electromagnetic fields in nanoscale volumes can induce a secondary process where plasmon oscillation resonates with the semiconductor band gap, that is, plasmonic resonant-energy transfer (PRET).[4] Recently, plasmonic driven processes (whether charge or energy transfer) have been the focus of intense research.[3,4] For example, Mubeen et al. reported a water-splitting device based on Au/TiO_2 in which all the charge carriers involved in the reaction were Au hot e^-.[2] Tailored composite materials and bimetallic plasmonic NPs have also shown high efficiency in driving extensive number of selective chemical reactions.[3,4]

In metal oxides that are used to convert solar light into chemical energy, the catalytic process is driven by transient changes in the metal oxide's properties, such as the metal oxidation state and/or the local reconstruction of catalytic sites. Pump-probe, time-resolved, and in operando X-ray spectroscopies[5] can detect such modifications by probing the local electronic and structural properties of a selected atomic species and shed light on key steps of the catalytic process, the knowledge thus gained can aid the design of efficient photocatalysts.

While many approaches that couple plasmonic NPs to semiconductors have been reported to date, less attention has been paid to the atomistic description of the trapping sites and the charge localization induced by excited carriers.

Long lifetimes (μs to ms) and close proximity to the surface are the essential requirements for photogenerated carriers to efficiently participate in chemical reactions. Acquiring spectra during continuous Au LSPR excitation enhances the sensitivity to variations caused by long lived-charges. A spectrum acquired under these conditions will be the average of the characteristic line-shapes of all the intermediate states, each weighted by its lifetime.

Variations relative to long-lived charges are then amplified with respect to carriers that rapidly recombine.

[*] Dr. L. Amidani, Prof. F. Boscherini
Department of Physics and Astronomy, University of Bologna
Viale Berti-Pichat 6/2, 40127 Bologna (Italy)
Dr. L. Amidani, Dr. P. Glatzel
ESRF—The European Synchrotron
71 Avenue des Martyres
Grenoble 38000 (France)
E-mail: lucia.amidani@esrf.fr
Dr. A. Naldoni, Dr. M. Marelli, Dr. V. Dal Santo
CNR-Istituto di Scienze e Tecnologie Molecolari
Via Golgi 19, 20133 Milano (Italy)
E-mail: a.naldoni@istm.cnr.it
Dr. M. Malvestuto
Elettra-Sincrotrone Trieste
S.S. 14 Km 163.5 Area Science Park Trieste, 34149 (Italy)

[**] The projects "TIMES: technology and materials for the efficient use of solar energy"—Accordo Quadro Regione Lombardia—CNR, the FIRB projects RBAP115AYN and RBFR13XLJ9 from MIUR, and project EX-PRO-REL (Elettra Sincrotrone Trieste) are gratefully aknowledged. This work was partially supported by EU within the FP7 project PASTRY (GA 317746). We acknowledge: J.-D. Cafun, S. Bauchau and J. Jacobs of the ESRF, Prof. E. Selli and F. Riboni for supplying N-TiO_2.

Supporting information for this article is available on the WWW under http://dx.doi.org/10.1002/anie.201412030.

Herein we report a XANES/RIXS investigation of TiO_2/Au powders during laser excitation of the LSPR of Au NPs. The spectral variations observed were significant and strongly support a laser-induced reduction of a small percentage of Ti atoms by long-lived hot electrons that remain trapped in Ti sites at the semiconductor surface after being injected from the Au NPs.

We measured powders of pure and N-doped TiO_2 (anatase) of 15 nm average size loaded with 10 wt% Au NPs of 5 nm mean diameter. Both UV/Vis absorption spectra (Figure S1 in the Supporting Information) show the Au LSPR band centered at about 550 nm. However, the absorption of N-TiO_2 extends to the visible spectrum reflecting its reduced band gap and yellow color.

In Figure 1 a a representative HRTEM image of TiO_2/Au shows the sharp interface between TiO_2 and Au NPs, a crucial morphological feature to assure an efficient Au–TiO_2 interaction.

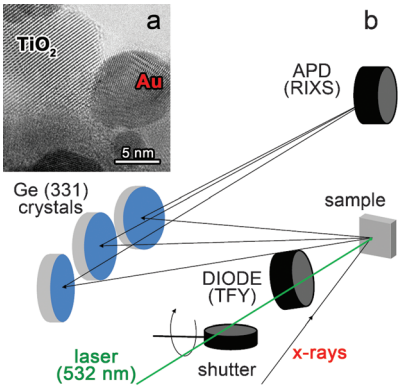

Figure 1. a) HRTEM images showing the sharp interface formed after Au NPs deposition on TiO_2 samples. b) Scheme of the experimental set-up.

The experiment was performed on the ID26 beamline at the ESRF[6] with the set-up shown schematically in Figure 1 b. We recorded RIXS, high energy resolution fluorescence detected (HERFD) and total fluorescence yield (TFY) XANES (see Supporting Information for details). Au NPs were excited with a 532 nm 200 mW continuous-wave laser and a shutter was used to alternately record laser on/laser off spectra.

Figure 2 shows laser effects on bare and Au-loaded TiO_2 in the pre-edge region measured in TFY. Average of laser off scans are in the top panel and show the typical line shape of anatase, with four features labeled A_{1-3} and B related to Ti 3d states.[7]

Laser on/laser off spectral differences are reported in the bottom panel of Figure 2. Laser irradiation leaves TiO_2 unchanged while inducing weak variations in N-TiO_2. As soon as Au NPs are added to oxides, large changes appear in the whole pre-edge region of TiO_2 and the features in N-TiO_2 are strongly enhanced. We recall that N-TiO_2 slightly absorbs at 532 nm because of the reduced band gap caused by N doping. The amplitude and shape of the differential signal is similar for the two powders, hence it cannot be related to

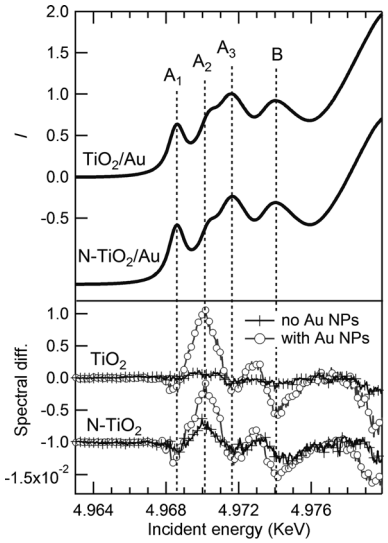

Figure 2. Top: TiO_2/Au and N-TiO_2/Au laser-off pre-edges measured in TFY. Bottom: laser-on/laser-off spectral differences on bare TiO_2/Au powders (line with vertical ticks) and plasmonic TiO_2/Au powders (line with empty circles).

PRET, which is energetically allowed only in N-TiO_2 and not in pure TiO_2.[4e] The laser induces a strong increase of A_2 (ca. 1.4%) and modulates the whole pre-edge region as seen by the oscillatory behavior of both differential signals. The line shape of the Ti pre-edge might be also affected by temperature variations.[8] We estimated the sample heating expected in our experimental conditions and found it negligible (see Supporting Information).[9] Therefore, we believe that the variations observed on the electronic structure of Ti are a consequence of hot e^- injection into the TiO_2 CB.

To understand what causes such variations, we focused on N-TiO_2 and recorded RIXS data. In Figure 3 we report the RIXS plane in the region of the K_β emission (1s3p RIXS) of N-TiO_2 pre-edge, where the four features A_{1-3} and B appear at different energies: A_3, B, and the main edge lie on the RIXS cut named HERFD-I (detection of K_β maximum) while

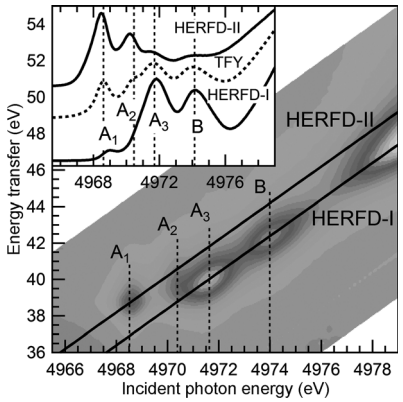

Figure 3. 1s3p RIXS plane of Ti K-edge pre-edge of N-TiO_2. 1s3p RIXS plane is obtained by collecting Ti K_β fluorescence while scanning the Ti K-edge with the incident X-ray beam. HERFD-I and HERFD-II cuts are shown with solid black lines. Inset: the pre-edge region of the Ti K-edge spectrum for N-TiO_2 measured in TFY, HERFD-I, and HERFD-II.

A_1 and A_2 peaks at lower emitted energies and can be isolated from the rest of the spectrum by acquiring HERFD-II.

The comparison of HERFD-I, HERFD-II, and TFY pre-edges is shown in the inset of Figure 3. TiO_2 pre-edge probes metal d states, directly through quadrupolar transitions or indirectly through dipole transitions to d–p hybridized states.[10] Although peak assignment has been debated at length, it can be stated that A_1 and A_3 probe mainly the t_{2g} band and A_2 and B the e_g. The separation of pre-edge peaks in different cuts of the RIXS plane reflects the effect of the core–hole potential, which in turn depends on the localization of the final states reached.[11a] A_1 and A_2 have thus been associated to transitions to states strongly localized on the absorber.[11] On the other hand, investigation of nanosized TiO_2 indicated that A_2 is particularly sensitive to crystallinity[12] and NP size[13] so that A_2 intensity can be correlated to low-coordinated Ti sites at the surface.

We used RIXS to decouple the laser effect on A_1 and A_2 from the rest of the spectrum by acquiring HERFD-I and HERFD-II spectra separately. Results on HERFD-I full XANES are shown in Figure 4 together with TFY acquired in parallel. Figure 4a shows laser-off spectra and Figure 4b the laser-induced spectral differences, which are significant in the pre-edge region while in the post-edge data essentially scatter around zero. Studies of TiO_2/dye composites for solar cells, support e^- injection from the dye to TiO_2 and recent studies have indicated low-coordinate Ti sites as e^- traps 100 ps after the injection, implying that a reduction of the Ti oxidation state is expected after trapping.[5c]

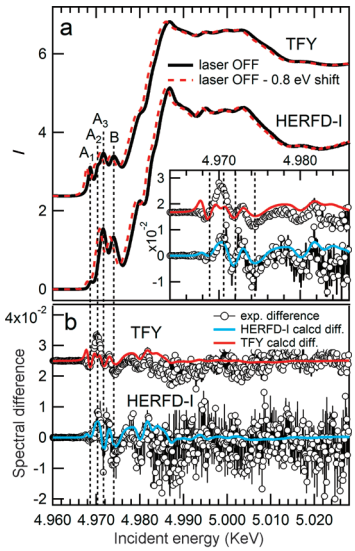

Figure 4. Effect of LSPR excitation on full XANES acquired in TFY and HERFD-I on N-TiO_2/Au. a) experimental (black continuous line) and red-shifted (red dashed line) laser-off spectra. b) TFY and HERFD-I laser-on/laser-off differences of experimental data (black dotted line) and generated shifted/unshifted differences of TFY (red line) and HERFD-I (blue line) spectra. The inset in (a) shows a magnification of the pre-edge region.

To verify if our results are consistent with an edge shift resulting from Ti reduction, we red-shifted laser-off TFY and HERFD-I scans and computed the difference between shifted/unshifted spectra. The differences are reported in Figure 4b. We tested red-shifts from 0 to −2 eV and found best agreement for −0.8 eV. The weight used to best match the experimental data is 0.74%.

The agreement is excellent, both the shape and amplitude of variations induced by hot e^- transfer are well reproduced over the whole XANES range. The agreement is also good for TFY XANES, but the mismatch in the A_1 and A_2 peaks indicated the need to separately investigate laser effects on HERFD-II.

Figure 5 shows laser-on/laser-off scans of HERFD-II and HERFD-I. The top panel shows laser-off spectra and their shifted counterpart for N-TiO_2/Au, while the bottom one displays laser on-laser off differences compared with 0.74% generated differences. The experimental results on HERFD-II are clearly not consistent with a red-shift, in this case the Au-TiO_2 interaction induces an increase of A_2 coupled with a slight decrease of A_1.

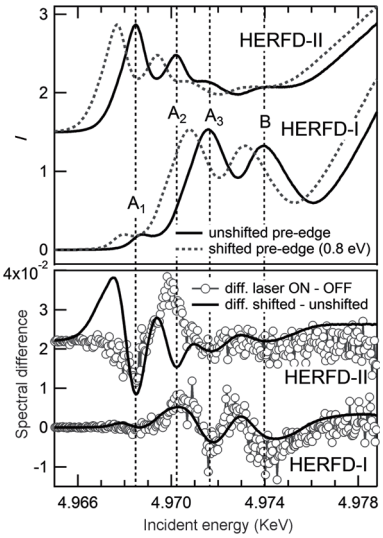

Figure 5. Top: experimental (solid line) and red-shifted (dashed line) laser-off HERFD-II and HERFD-I pre-edges of N-TiO_2/Au. Bottom: experimental laser-on/laser-off differences (line with empty circles) and the generated shifted/unshifted differences (solid black line) for HERFD-II and HERFD-I. HERFD-I laser variations are reproduced fairly well by red-shifting the experimental data. In contrast, HERFD-II laser variations are not compatible with a red-shift of transitions.

The red-shift of HERFD-I is consistent with the presence of extra-charge in the vicinity of a small percentage of Ti atoms, since the main parameter affecting transitions to states with *p* character (edge and dipolar pre-edge peaks) is the change in the valence electron distribution around metal atoms.[14] On the other hand, in HERFD-II the presence of extra charge does not shift A_1 and A_2, we think because the injected charge is not confined in these strongly localized orbitals. However, the pronounced increase of A_2 recalls the effect on the pre-edge of low-coordinate Ti sites at the

surface, characterized by extra-charge as a result of dangling bonds or structural distortions.[13] The twofold behavior observed in our data is therefore the signature of long-lived electrons that after injection remain trapped in d–p states[10] of Ti atoms at the surface and appear as new laser-induced low-coordinate Ti sites. Based on our results, the conversion efficiency of photons absorbed into surface-trapped electrons is approximately 0.1 % (see Supporting Information).

Interactions between molecules and the TiO_2 surface play a key role in photocatalytic processes, such as water splitting and synthesis of fine chemicals. Defective sites, because of the absence of some chemical bonds, present local extra charge and partial structural rearrangement which favor the adsorption of small molecules in their vicinity compared to stoichiometric surface regions. In addition, in metal NPs supported on oxides, the interface clearly plays a critical role providing enhanced reactivity.[15] Similarly, we suggest that in plasmonic TiO_2/Au, hot e^- remain trapped near the composite interface in Ti d–p states and generate sites with a similar electronic and structural nature to the already existing low-coordinate ones therefore acting as additional sites for the adsorption of molecule and providing photogenerated charges to start the catalytic reaction.

In conclusion, with synchrotron-based XAS and RIXS we provided atomistic insights into the electronic and structural localization of plasmonic-generated charges. Our investigation indicates that part of the injected electrons survive longer, being captured at Ti sites concentrated near the surface. These Ti site have all the characteristics required to be active sites in plasmonic photocatalysis.

Keywords: hot electrons · photocatalysis · plasmon resonance · titanium · X-ray absorption spectroscopy

How to cite: *Angew. Chem. Int. Ed.* **2015**, *54*, 5413–5416
Angew. Chem. **2015**, *127*, 5503–5506

[1] a) M. Grätzel, *Nature* **2001**, *414*, 338–344; b) Z. Li, W. Luo, M. Zhang, J. Feng, Z. Zou, *Energy Environ. Sci.* **2013**, *6*, 347–370; c) M. Marelli, A. Naldoni, A. Minguzzi, M. Allieta, T. Virgili, G. Scavia, S. Recchia, R. Psaro, V. Dal Santo, *ACS Appl. Mater. Interfaces* **2014**, *6*, 11997–12004.

[2] S. Mubeen, J. Lee, N. Singh, S. Kraemer, G. D. Stucky, M. Moskovits, *Nat. Nanotechnol.* **2013**, *8*, 247–251.

[3] a) S. Linic, P. Christopher, D. B. Ingram, *Nat. Mater.* **2011**, *10*, 911–921; b) C. Clavero, *Nat. Photonics* **2014**, *8*, 95–103; c) X. Huang, Y. Li, Y. Chen, H. Zhou, X. Duan, Y. Huang, *Angew. Chem. Int. Ed.* **2013**, *52*, 6063–6067; *Angew. Chem.* **2013**, *125*, 6179–6183; d) Y. Sugano, Y. Shiraishi, D. Tsukamoto, S. Ichikawa, S. Tanaka, T. Hirai, *Angew. Chem. Int. Ed.* **2013**, *52*, 5295–5299; *Angew. Chem.* **2013**, *125*, 5403–5407.

[4] a) Y. Tian, T. Tatsuma, *Chem. Commun.* **2004**, 1810–1811; b) A. Furube, L. Du, K. Hara, R. Katoh, M. Tachiya, *J. Am. Chem. Soc.* **2007**, *129*, 14852–14853; c) Y. Tian, T. Tatsuma, *J. Am. Chem. Soc.* **2005**, *127*, 7632–7637; d) Z. Liu, W. Hou, P. Pavaskar, M. Aykol, S. B. Cronin, *Nano Lett.* **2011**, *11*, 1111–1116; e) S. K. Cushing, J. Li, F. Meng, T. R. Senty, S. Suri, M. Zhi, M. Li, A. D. Bristow, N. Wu, *J. Am. Chem. Soc.* **2012**, *134*, 15033–15041; f) R. Long, K. Mao, M. Gong, S. Zhou, J. Hu, M. Zhi, Y. You, S. Bai, J. Jiang, Q. Zhang, X. Wu, Y. Xiong, *Angew. Chem. Int. Ed.* **2014**, *53*, 3205–3209; *Angew. Chem.* **2014**, *126*, 3269–3273; g) J. S. DuChene, B. C. Sweeny, A. C. Johnston-Peck, D. Su, E. A. Stach, W. D. Wei, *Angew. Chem. Int. Ed.* **2014**, *53*, 7887–7891; *Angew. Chem.* **2014**, *126*, 8021–8025.

[5] a) A. Minguzzi, O. Lugaresi, E. Achilli, C. Locatelli, A. Vertova, P. Ghigna, S. Rondinini, *Chem. Sci.* **2014**, *5*, 3591–3597; b) H. G. Sanchez Casalongue, M. Ling Ng, S. Kaya, D. Friebel, H. Ogasawara, A. Nilsson, *Angew. Chem. Int. Ed.* **2014**, *53*, 7169–7172; *Angew. Chem.* **2014**, *126*, 7297–7300; c) M. H. Rittmann-Frank, C. J. Milne, J. Rittmann, M. Reinhard, T. J. Penfold, M. Chergui, *Angew. Chem. Int. Ed.* **2014**, *53*, 5858–5862; *Angew. Chem.* **2014**, *126*, 5968–5972.

[6] C. Gauthier, V. Sole, R. Signorato, J. Goulon, E. Moguiline, *J. Synchrotron Radiat.* **1999**, *6*, 164–166.

[7] L. A. Grunes, *Phys. Rev. B* **1983**, *27*, 2111–2131.

[8] a) O. Durmeyer, E. Beaurepaire, J.-P. Kappler, C. Brouder, F. Baudelet, *J. Phys. Condens. Matter* **2010**, *22*, 125504–125509; b) C. Brouder, D. Cabaret, A. Juhin, P. Sainctavit, *Phys. Rev. B* **2010**, *81*, 115125–115130.

[9] A. O. Govorov, H. Richardson, *Nanotoday* **2007**, *2*, 30–38.

[10] T. Yamamoto, *X-ray Spectrom.* **2008**, *37*, 572–584.

[11] a) P. Glatzel, M. Sikor, M. Fernández-García, *Eur. Phys. J. Special Topics* **2009**, *169*, 207–214; b) Y. Joly, D. Cabaret, H. Renevier, C. R. Natoli, *Phys. Rev. Lett.* **1999**, *82*, 2398–2401; c) J. Szlachetko, J. Sá, *CrystEngComm* **2013**, *15*, 2583–2587.

[12] a) T. L. Hanley, V. Luca, I. Pickering, R. F. Howe, *J. Phys. Chem. B* **2002**, *106*, 1153–1160; b) S. J. Stewart, M. Fernández-García, C. Belver, B. Simon Mun, F. G. Requejo, *J. Phys. Chem. B* **2006**, *110*, 16482–16486.

[13] a) V. Luca, *J. Phys. Chem. C* **2009**, *113*, 6367–6380; b) X. Chen, T. Rajh, Z. Wang, M. C. Thurnauer, *J. Phys. Chem. B* **1997**, *101*, 10688–10697.

[14] A. H. de Vries, L. Hozoi, R. Broer, *Int. J. Quantum Chem.* **2003**, *91*, 57–61.

[15] a) M. Cargnello, V. V. T. Doan-Nguyen, T. R. Gordon, R. E. Diaz, E. A. Stach, R. J. Gorte, P. Fornasiero, C. B. Murray, *Science* **2013**, *341*, 771–773.

Received: December 15, 2014
Published online: March 6, 2015

